# Aeration, Flow Instabilities, and Residual Energy on Pooled Stepped Spillways of Embankment Dams

Stefan Felder, Ph.D.[1]; and Hubert Chanson[2]

**Abstract:** Air-water flow experiments were conducted on some flat and pooled stepped spillways with slopes of 8.9° and 26.6° in transition and skimming flows. The study comprised the observations of the flow patterns, characteristic air-water flow properties, and energy dissipation performances. The air-water flow properties showed some differences in terms of interfacial velocity, bubble count rate, and turbulence intensity between the stepped chutes for the two channel slopes. These differences were also reflected in the residual energy data, highlighting a better energy dissipation rate for the pooled stepped spillway with slope of 8.9°. However, the aerated flows on the pooled stepped spillways exhibited some hydrodynamic instabilities, and a safe operation must be tested in physical models. The flat stepped spillway appeared to be the preferable design in terms of energy dissipation and flow stability. **DOI: 10.1061/(ASCE)IR.1943-4774.0000627.** 

**CE Database subject headings:** Spillways; Flow patterns; Flow resistance; Embankment dams.

**Author keywords:** Pooled stepped spillways; Flow aeration; Pulsating flow; Instationary flow patterns; Residual energy; Flow resistance.

## Introduction

A hydraulic structure must be designed to discharge water safely, avoiding any damage to the structure and surroundings. The release facility must safely dissipate the kinetic energy of the flow to avoid damage of the reach just downstream. One type of hydraulic structure is the stepped spillway, which is characterized by a large energy dissipation rate above the staircase chute. The design of stepped spillways has been known for at least 3,500 years (Chanson 2001). With the development of a new, more efficient construction technique [roller compacted concrete (RCC)], the design of stepped spillways regained some interest in the 1970s and 1980s (Hansen and Reinhardt 1991; Chanson 2001; Ditchey and Campbell 2000). Today, the stepped spillway design is commonly used in hydraulic structures with a wide range of applications, including flood release facilities and overflow weirs of embankment and gravity dams. Stepped chutes are mostly equipped with flat horizontal steps of uniform step height. In some cases, the steps may be equipped with a weir at the step edge, creating a pool. Pooled stepped spillways are known for large energy dissipation performance as well as some instable flow conditions for some discharges (Thorwarth 2008). Experiments on pooled stepped spillways were conducted in the last decade to provide a better understanding of the flow properties and energy dissipation performances (Kökpinar 2004; André 2004; Thorwarth 2008; Takahashi et al. 2008; Felder et al. 2012a, b). Thorwarth (2008) highlighted some self-induced instabilities on pooled stepped spillways with slopes of 8.9° and 14.6° with various pool weir heights.

In the present study, the air-water flow properties on pooled stepped spillways with slopes of 8.9° and 26.6° were investigated with a ratio of pool weir height to step length $w/l = 1{:}6.45$. The air-water flow experiments provided some new insights into the energy dissipation and aeration performances and some instationary flow processes.

## Stepped Spillway Facilities, Instrumentation, and Experimental Flow Conditions

Experiments were conducted on two different large-scale stepped spillway models equipped with flat and pooled steps (Table 1). Table 1 summarizes the experimental facilities with channel slopes of $\theta = 26.6°$ and $\theta = 8.9°$. On the stepped chutes with $\theta = 26.6°$, a smooth inflow was created from an upstream intake basin and a contraction ratio of 4.23:1 through a broad-crested weir. The discharge was controlled and calibrated by the broad-crested weir (Felder and Chanson 2012a).

For the stepped spillways with $\theta = 8.9°$, a uniform discharge was provided through an upstream stilling tank followed by an uncontrolled broad-crested weir. At the downstream end, a sharp-crested weir was used for the discharge measurements using an acoustic displacement meter. The experimental setup was previously used by Thorwarth (2008) to investigate flow instabilities on pooled stepped chutes with slopes of 8.9° and 14.6°. However, Thorwarth (2008) did not systematically research the air-water flow properties, and the present experiments added some important novelties for the stepped spillways with $\theta = 8.9°$. Further details on the experimental configurations are listed in Table 1, and a sketch of the stepped configurations is provided in Fig. 1. Herein the ratio of pool weir height to step length $w/l = 0.155$ was about the same for both pooled stepped facilities.

The experiments were performed for a broad range of discharges per unit width $q_w$ (Table 1). In both facilities, the air-water flow measurements were conducted in transition and skimming flows with double-tip conductivity probes of similar designs

[1]School of Civil Engineering, Univ. of Queensland, Brisbane QLD 4072, Australia (corresponding author). E-mail: stefan.felder@uqconnect.edu.au

[2]Professor, School of Civil Engineering, Univ. of Queensland, Brisbane QLD 4072, Australia. E-mail: h.chanson@uq.edu.au

Note. This manuscript was submitted on December 6, 2012; approved on April 17, 2013; published online on April 19, 2013. Discussion period open until March 1, 2014; separate discussions must be submitted for individual papers. This paper is part of the ***Journal of Irrigation and Drainage Engineering***, Vol. 139, No. 10, October 1, 2013. © ASCE, ISSN 0733-9437/2013/10-880-887/$25.00.

**Table 1.** Summary of Experimental Configurations and Flow Conditions for the Flat and Pooled Stepped Spillways

| Slope | $W$ (m) | Steps | $h$ (m) | $w$ (m) | $l_w$ (m) | Conductivity probe | $q_w$ (m$^2$/s) | $d_c/h$ | R | $w/l$ | $w/h$ |
|---|---|---|---|---|---|---|---|---|---|---|---|
| 26.6° | 0.52 | 10 flat | 0.1 | N/A | N/A | Double-tip ($\varnothing = 0.25$ mm) | 0.008–0.262 | 0.18–1.91 | $3.1 \times 10^4$–$1.0 \times 10^6$ | N/A | N/A |
| | | 9 pooled | | 0.031 | 0.015 | $\Delta x = 7.2$ mm, $\Delta z = 2.1$ mm | 0.004–0.267 | 0.11–1.94 | $1.5 \times 10^4$–$1.1 \times 10^6$ | 0.155 | 0.31 |
| 8.9° | 0.5 | 21 flat | 0.05 | N/A | N/A | Double-tip ($\varnothing = 0.13$ mm) | 0.004–0.234 | 0.24–3.54 | $3.4 \times 10^4$–$9.3 \times 10^5$ | N/A | N/A |
| | | 20 pooled | | 0.05 | 0.015 | $\Delta x = 5.1$ mm, $\Delta z = 1$ mm | 0.009–0.234 | 0.39–3.54 | $3.4 \times 10^4$–$9.3 \times 10^5$ | 0.157 | 1.0 |

(Table 1). The air-water flow measurements were conducted for Reynolds numbers covering more than one order of magnitude with $R > 10^5$ typically to minimize potential scale effects. For all experiments, the air-water flow measurements were sampled for 45 s at 20 kHz per sensor. The raw voltage data were analyzed with the same data analysis software. More details about the facilities, instrumentation, and the data analysis software are detailed by Felder (2013).

## Visual Observations of Flow Patterns, Flow Regimes, and Flow Instabilities

Some detailed visual observations were conducted for all stepped configurations including the flow patterns, the changes in flow regimes, and the inception point of free-surface aeration.

For the flat steps for both channel slopes, a nappe flow regime existed, exhibiting typical flow patterns with free-falling jets from one step to the next for the smallest flow rates (i.e., $d_c/h \leq 0.95$ for $\theta = 8.9°$ and $d_c/h \leq 0.57$ for $\theta = 26.6°$) (Toombes 2002; Toombes and Chanson 2008). With increasing discharges (i.e., $0.95 \leq d_c/h \leq 1.69$ for $\theta = 8.9°$ and $0.57 \leq d_c/h \leq 0.9$ for $\theta = 26.6°$), the flow showed some strong splashing in the transition flow regime. For the 8.9° slope, no air cavities were observed in the step niches, whereas the flow on the 26.6° slope showed some characteristic flapping mechanism with some cavity air pockets. For the largest flow rates, a skimming flow regime existed with stable recirculation movements in the step cavities. The surface was parallel to the pseudobottom formed by the step edges for $\theta = 26.6°$. For the 8.9° slope, the free-surface was not completely parallel to the pseudobottom and some pseudoundular free-surface profiles were observed as previously reported on a 3.4° stepped chute (Chanson and Toombes 2002a). The amount of entrained air appeared smaller for the stepped chute with $\theta = 8.9°$, possibly linked with the different cavity shape.

### *Nappe Flow Regime on Pooled Stepped Spillways*

For both channel slopes, the nappe flow consisted of free-falling nappes impacting the underlying nappe pool filled with water. Some air was entrained into the pool by the plunging jet and detrained before the next overfall. The nappe flows for the 8.9° slope pooled steps appeared very stable for $d_c/h < 1.08$. For the 26.6° sloped spillway, the nappe flow regime existed for discharges $d_c/h < 0.45$. For a range of the nappe flow rates on the 26.6° stepped chute (i.e., $0.3 < d_c/h < 0.45$), some pulsations were observed in the first step cavity leading to some small instabilities of the free-falling nappes (Fig. 2). During the pulsations, some small

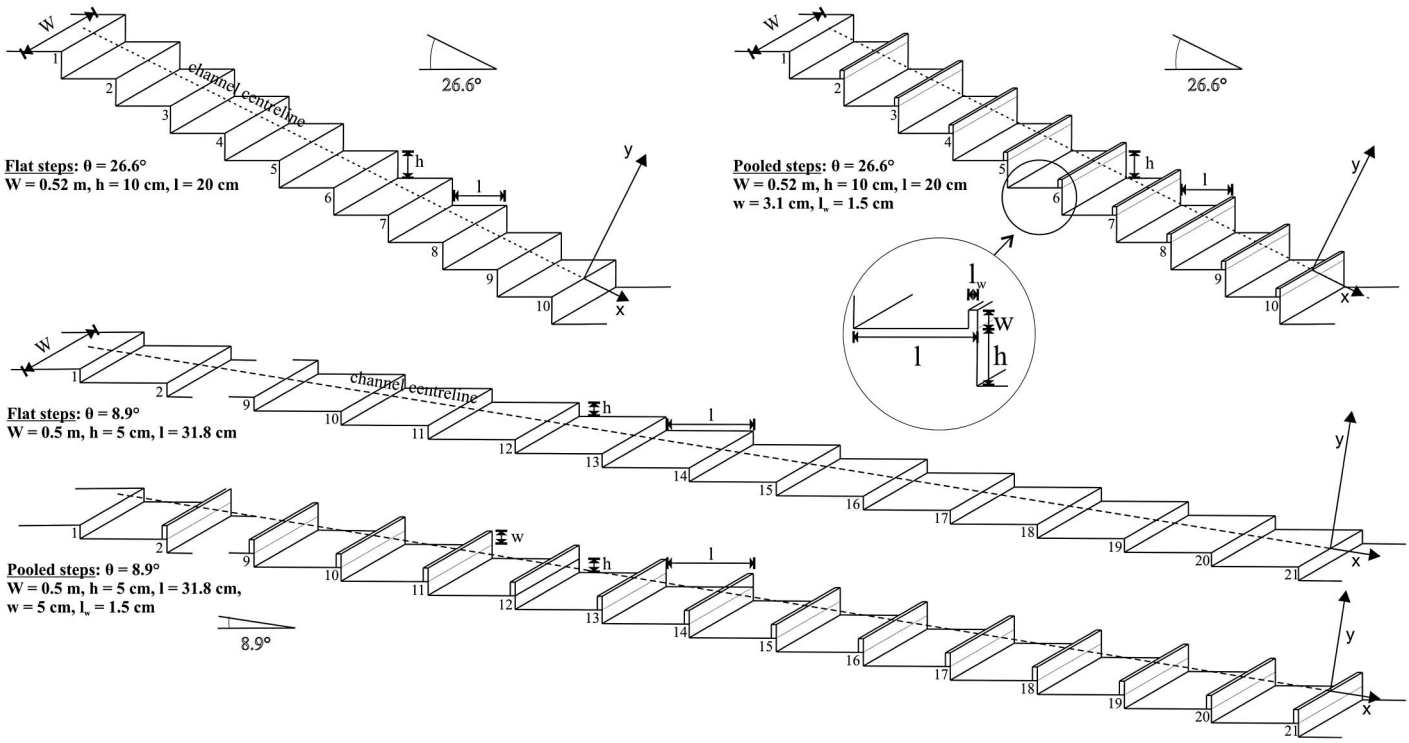


**Fig. 1.** Sketch of flat and pooled stepped spillways in the present study; definition of first vertical measurement position on flat and pooled steps ($y = 0$); note the missing steps between steps 2 and 9 in the drawing for $\theta = 8.9°$ for better clarity

**Fig. 2.** Instabilities caused by some pulsating flows in first step cavity in nappe flow regime on the pooled stepped spillway ($\theta = 26.6°$): $d_c/h = 0.40$, $q_w = 0.025$ m$^2$/s, $\mathsf{R} = 1.0 \times 10^5$ (chronological photo order from left to right and top to bottom)

waves were ejected from the first step cavity and caused some deviations of the lengths of the nappes. With every pulsation, the nappe impact shifted from the next step cavity to one step further downstream (Fig. 2). For the lower boundary of the pulsating flow rates ($d_c/h = 0.3$), the pulsations appeared about every second and at the upper boundary ($d_c/h = 0.45$) every 5 s. The pulsating flow was quasi-periodic for all flow rates. Similar nappe flow patterns on a pooled stepped spillway with $\theta = 30°$ were reported by Takahashi et al. (2008).

### *Transition Flow Regime on Pooled Stepped Spillways*

For intermediate flow rates, a transition flow regime was observed for both pooled configurations. For the pooled chute with $\theta = 26.6°$, some strong splashing in the air-water flow region downstream of the inception point of free-surface aeration was found for $0.45 < d_c/h < 0.97$. No pulsations in the first step cavity were present, and the transition flow appearance was comparable to typical observations on the flat stepped spillway with some small instabilities in the air-water flows. For the 8.9° sloped pooled stepped spillway, the transition flow regime exhibited much stronger instabilities for $1.08 < d_c/h < 1.76$. These instabilities caused some significant flow disturbances, including jump waves propagating downstream (Fig. 3). The occurrence of jump waves was associated with a number of unstable mechanisms, including a partial hydraulic jump in the pooled cavity, the random ejection of air-water flows from the cavity, and some strong instability at the free-surface. Fig. 3 illustrates some typical jump waves for a transition flow discharge. The frequencies of the jump waves were about 0.25–0.4 Hz. Some waves were caused by some pulsating clear-water flows in the first step pool downstream of the broad-crested weir. The pulsations initiated jump waves every 6–8 s. The pulsations caused every second jump wave to propagate downstream. The other waves seemed to be initiated by further instationaries in the first few stepped pools. With increasing discharges, the instabilities appeared to decrease in size. The present findings were in agreement with the investigations by Thorwarth (2008) in the same pooled stepped spillway facility with slopes of 8.9° and 14.6° and a range of pool weir heights.

### *Skimming Flow Regime on Pooled Stepped Spillways*

For the largest flow rates (i.e., $d_c/h > 0.97$ for $\theta = 26.6°$ and $d_c/h > 1.76$ for $\theta = 8.9°$), a skimming flow regime was observed. For the 26.6° pooled stepped spillway, the flow patterns were comparable with the flat stepped chute with some stable air-water cavity recirculation downstream of the inception point of air entrainment. The flow depth was larger, however, because of the pool weir height. For the 8.9° sloped pooled chute, the skimming flow appeared less stable than that on the flat stepped spillway. Some strong free-surface fluctuations were visible upstream of the inception point of free-surface aeration linked with the increased step roughness induced by the weir pools. Furthermore, some instable cavity recirculation and ejection processes were seen for all skimming flow discharges in the present study (Fig. 4).

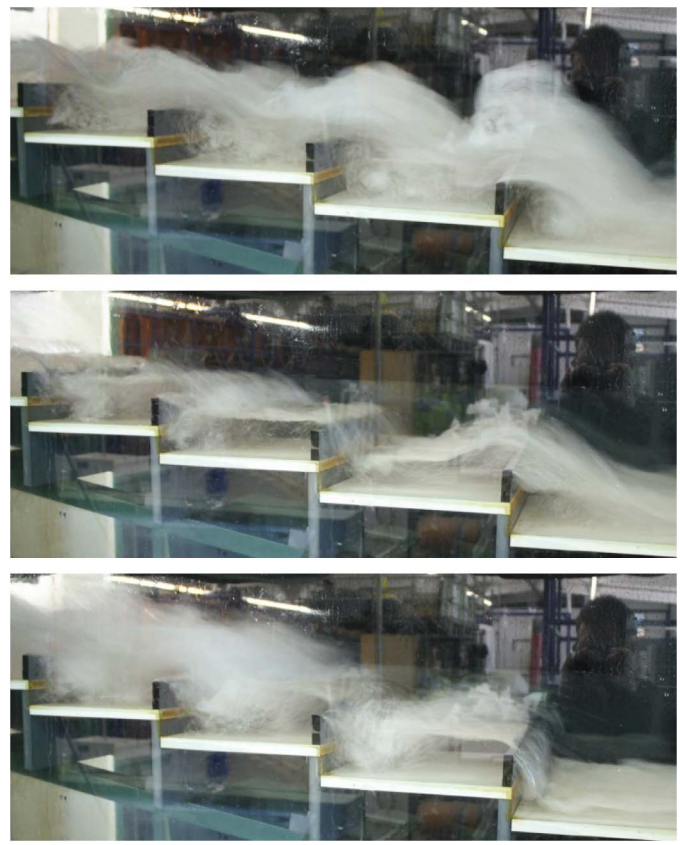

**Fig. 3.** Jump waves in the transition flow regime on the pooled stepped spillway ($\theta = 8.9°$): $d_c/h = 1.20$; $q_w = 0.046$ m$^2$/s; $\mathsf{R} = 1.8 \times 10^5$

**Fig. 4.** Instabilities in the skimming flow regime on the pooled stepped spillway ($\theta = 8.9°$): $d_c/h = 2.66$; $q_w = 0.152$ m$^2$/s; R $= 6.0 \times 10^5$

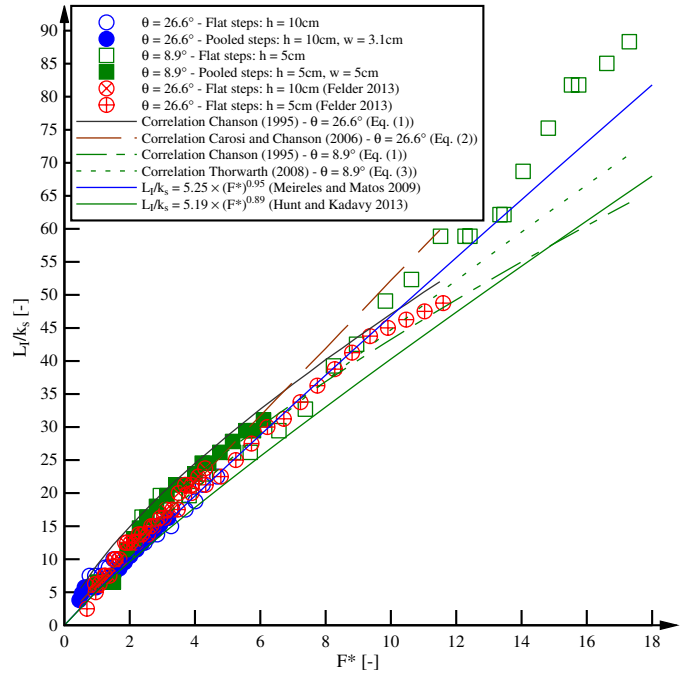


**Fig. 5.** Locations of inception point of free-surface aeration for the flat and pooled stepped spillways; comparison with empirical correlations [Eqs. (1)–(3)] and data with same channel slope by Felder (2013); transition and skimming flow data

Fig. 4 shows an example of instabilities for a typical skimming flow discharge including unstable cavity recirculation, sudden cavity ejections, and surface waves. These instabilities appeared to decrease with increasing discharges, but they were still present for the maximum flow rate in the present study ($d_c/h = 3.55$). Through visual observations and video documentation, the unstable processes had characteristic frequencies in the range of 0.5 to 2 Hz. Thus, the frequency range was similar to the observations in the transition flow regime and its unstable jump waves.

### Discussion

The comparison of the instationary flow processes on the pooled stepped spillways with different channel slopes highlighted the occurrence of pulsations in the first pooled step cavity and some associated flow instabilities. The pulsations occurred for different discharges and flow regimes, and the instationary flows on the 8.9° slope were much more significant. The experiments with two different slopes and different step and pool weir heights, respectively, suggest that any change of the cavity dimensions had impacts on the instability mechanisms and their characteristic frequencies. Furthermore, the changes in flow regimes showed some significant differences between the two channel slopes.

### Comparison of Locations of Inception Point of Free-Surface Aeration

The locations of inception points of free-surface aeration were observed in some detailed visual observations, and a comparison showed little difference (Fig. 5). Fig. 5 illustrates the inception point location for all configurations in the present study and some further data for flat stepped spillways with $\theta = 26.6°$ with channel width $W = 1$ m and step height $h = 10$ and 5 cm, respectively (Felder 2013). All data were in good agreement and were well correlated by some empirical equations for flat stepped chutes:

$$\frac{L_I}{k_s} = 9.719 \times (\sin\theta)^{0.0796} \times \mathrm{F}^{*0.713} \quad 27° \le \theta \le 53° \qquad (1)$$

$$\frac{L_I}{k_s} = 1.05 + 5.11 \times \mathrm{F}^* \quad \theta = 21.8°; \quad 0.45 \le d_c/h \le 1.6 \qquad (2)$$

and for pooled stepped chutes:

$$\frac{L_I}{k_s} = 9.7 \times (\sin\theta)^{0.23} \times \mathrm{F}^{*0.85} \quad \theta = 8.9° \text{ and } 14.6°; \quad 0.5 \le d_c/h \le 3.6 \qquad (3)$$

where $L_I$ = distance from the first step edge to the inception point; and F$^*$ = Froude number expressed in terms of the step roughness:

$$\mathrm{F}^* = \frac{q_w}{\sqrt{g \times \sin\theta \times k_s^3}} \qquad (4)$$

where $q_w$ = discharge per unit width; $g$ = gravity acceleration constant; and $k_s$ the step cavity height normal to the mainstream flow: $k_s = h \times \cos\theta$ for flat steps and $k_s = (h + w) \times \cos\theta$ for pooled steps. Overall there was a good agreement between experimental data and empirical correlations even though some equations were used out of their limits of application (Fig. 5). Some small differences were visible for the largest flow rates on the flat stepped chute with $\theta = 8.9°$, which might be linked with some subjective judgement of the exact location of the inception point. The observations by André (2004) on flat and pooled stepped spillways with $\theta = 30°$ also showed a good agreement of the inception points for both configurations. The present data were also compared with further empirical correlation of inception points on flat stepped spillways (Fig. 5). Although there was good agreement of the present data with the correlation by Meireles and Matos (2009) for flat steps with $16° \le \theta \le 26.6°$ and $1.9 \le \mathrm{F}^* \le 10$, some small deviations were observed with

the empirical correlation by Hunt and Kadavy (2013) valid for $14° \leq \theta \leq 18.4°$ and $0.1 \leq F^* \leq 28$ (Fig. 5).

## Comparison of Air-Water Flow Properties on Flat and Pooled Stepped Spillways

For all stepped spillways, the air-water flow properties were measured at step edges downstream of the inception point on the channel centerline for a range of discharges ($0.073 \leq q_w \leq 0.25$ m$^2$/s for $\theta = 26.6°$ and $0.054 \leq q_w \leq 0.234$ m$^2$/s for $\theta = 8.9°$). Some typical air-water flow properties in skimming flows are presented with a focus on some differences between the air-water flows on flat and pooled stepped chutes and between different channel slopes, respectively. A comparison of further macro- and microscopic air-water flow properties is provided in Felder (2013).

The void fraction distributions were in good agreement for both flat and pooled stepped spillways. Fig. 6(a) illustrates some 26.6° stepped chute data and Fig. 6(b) shows some 8.9° channel slope data. The data are presented with the void fraction distributions as functions of $y/Y_{90}$, where $Y_{90}$ is the distance perpendicular to the mainstream flow where $C = 90\%$. All void fraction distributions showed some S-shapes in good agreement with the advective diffusion equation solution (Chanson and Toombes 2002b):

$$C = 1 - \left(\tan h^2\left(K' - \frac{y/Y_{90}}{2 \times D_o}\right) + \frac{(y/Y_{90} - 1/3)^3}{3 \times D_o}\right) \quad (5)$$

where $K'$ = integration constant; and $D_o$ = function of the mean air concentration $C_{mean}$ only:

$$K' = K^* + 1/2 \times D_o - 8/81 \times D_o \quad (6)$$

$$C_{mean} = 0.7622 \times [1.0434 - \exp(-3.614 \times D_o)] \quad (7)$$

where $K^*$ = dimensionless constant; and the mean air-concentration $C_{mean}$ characterizes the depth-averaged air content in terms of $Y_{90}$: $C_{mean} = 1 - d/Y_{90}$ where $d$ = equivalent clear water flow depth.

A close agreement was achieved also in terms of the dimensionless interfacial velocity distributions $V/V_{90}$ for the flat and pooled steps for the respective channel slopes (Fig. 6), where $V_{90}$ = velocity where $C = 90\%$. All velocity distributions were correlated by a power law with exponent about $1/N = 1/10$ for $y/Y_{90} < 1$ and with uniform profiles above:

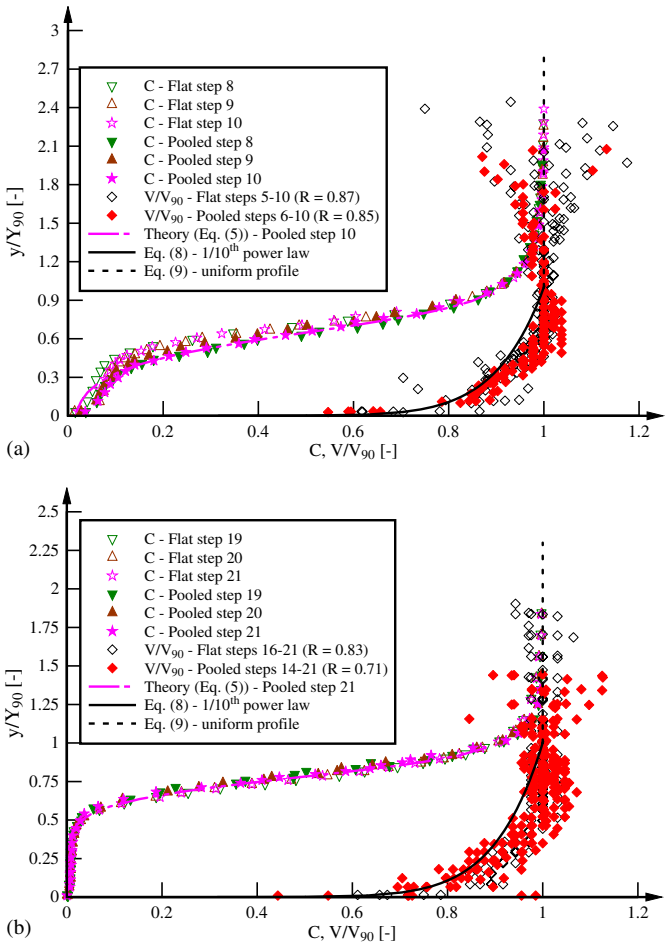


**Fig. 6.** Comparison of dimensionless distributions of void fraction and interfacial velocity $V/V_{90}$ on the flat and pooled stepped spillways; comparison with self-similarity equations [Eqs. (5), (8), and (9)]; legend contains correlation coefficients between interfacial velocity data and Eq. (8): (a) $\theta = 26.6°$: $d_c/h = 0.96$; $q_w = 0.094$ m$^2$/s; $R = 3.7 \times 10^5$; skimming flows; (b) $\theta = 8.9°$: $d_c/h = 2.66$; $q_w = 0.152$ m$^2$/s; $R = 6.0 \times 10^5$; skimming flows

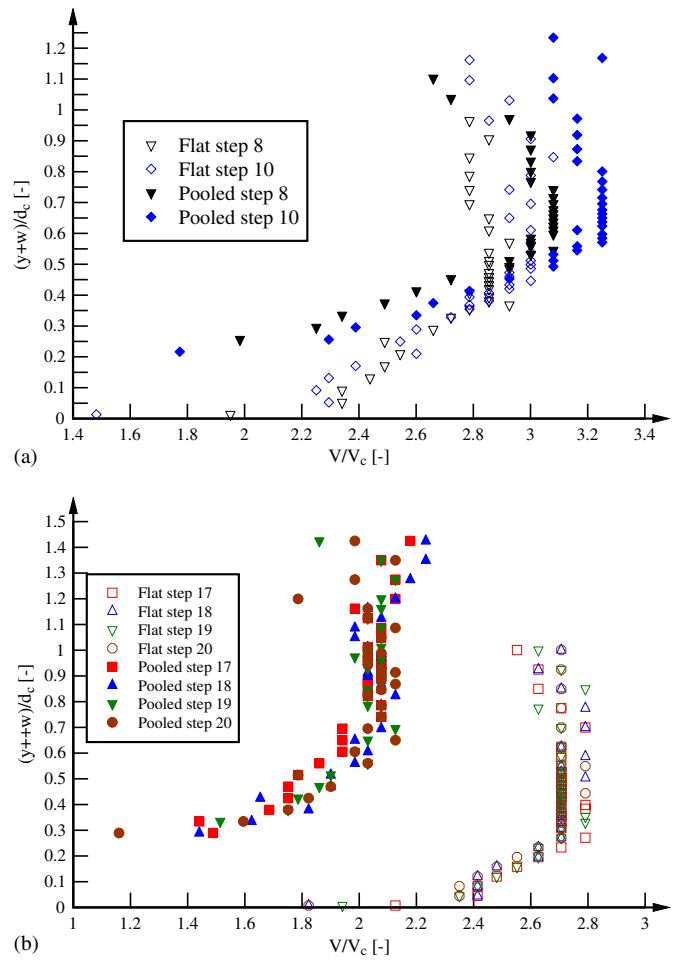


**Fig. 7.** Comparison of dimensionless distributions of interfacial velocity $V/V_c$ on the flat and pooled stepped spillways: (a) $\theta = 26.6°$: $d_c/h = 1.52$; $q_w = 0.187$ m$^2$/s; $R = 7.4 \times 10^5$; skimming flows; (b) $\theta = 8.9°$: $d_c/h = 2.66$; $q_w = 0.152$ m$^2$/s; $R = 6.0 \times 10^5$; skimming flows

$$\frac{V}{V_{90}} = \left(\frac{y}{Y_{90}}\right)^{1/N} \qquad y/Y_{90} < 1 \tag{8}$$

$$\frac{V}{V_{90}} = 1 \qquad y/Y_{90} \geq 1 \tag{9}$$

The correlation coefficients between the interfacial velocity data and Eq. (8) are added to Fig. 6 for both flat and pooled steps. Fig. 6 highlights some self-similarity of both void fraction and interfacial velocity profiles independently of the channel slope and flat and pooled step configuration.

Some differences, however, were observed in a different illustration of the dimensionless interfacial velocity $V/V_c$ as a function of $(y+w)/d_c$, where $V_c$ and $d_c$ are the critical velocity and depth, respectively (Fig. 7). For the pooled stepped chute, a translation by $w/d_c$ is seen for better illustration. For both channel slopes, some velocity differences were observed between the flat and pooled step configurations. For the 26.6° slope chute, the velocity was larger on the pooled step configuration [Fig. 7(a)] than on the flat steps. For the 8.9° sloped spillway, however, the velocity was smaller on the pooled stepped spillway than on the flat steps [Fig. 7(b)]. The contrasted finding between the two slopes is important because it suggests different energy dissipation performances for flat and pooled steps between the two channel slopes.

Some differences between flat and pooled stepped spillways were also observed in terms of the dimensionless bubble count rate $F \times d_c/V_c$ and turbulence intensity Tu (Fig. 8). For the stepped chute with $\theta = 26.6°$, the bubble count rate distributions showed a larger number of entrained air bubbles for the flat stepped spillway for all flow rates and at all step edges, whereas the turbulence levels for the flat and pooled steps were in close agreement [Fig. 8(a)]. For the 8.9° slope stepped chute, some larger bubble count rates were also observed for the flat steps, and some significantly larger turbulence levels were recorded for the pooled stepped spillway [Fig. 8(b)]. The large turbulence fluctuations seemed to be linked with the instationary flow processes on the pooled stepped spillway as shown by Felder and Chanson (2012b).

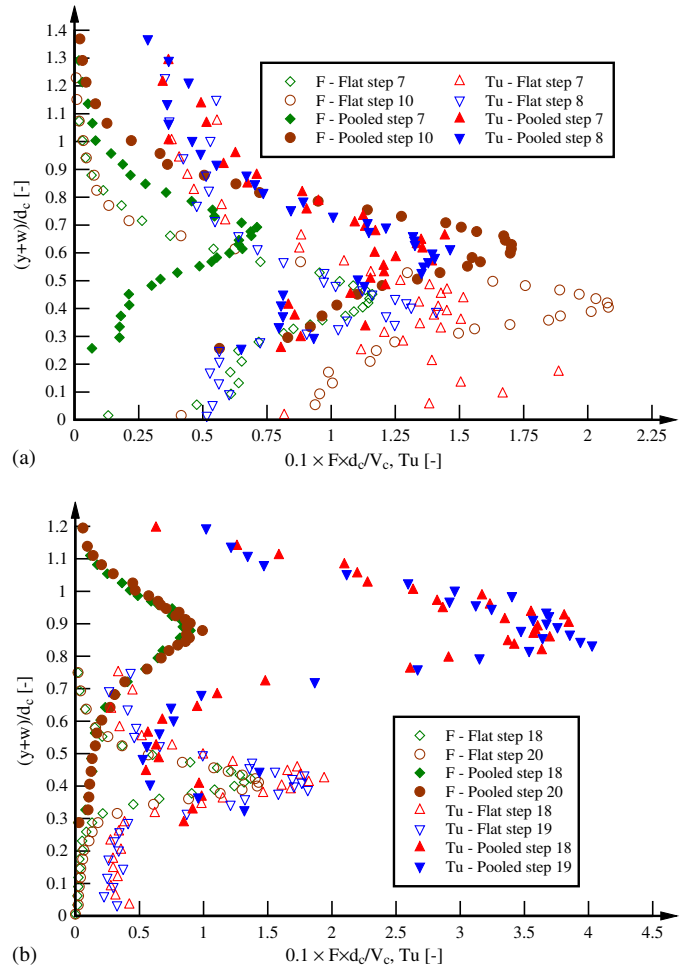


**Fig. 8.** Comparison of dimensionless bubble count rate and turbulence intensity distributions on the flat and pooled stepped spillways: (a) $\theta = 26.6°$: $d_c/h = 0.96$; $q_w = 0.094$ m$^2$/s; R $= 3.7 \times 10^5$; skimming flows; (b) $\theta = 8.9°$: $d_c/h = 3.55$; $q_w = 0.234$ m$^2$/s; R $= 9.3 \times 10^5$; skimming flows

## Residual Energy and Flow Resistance on Pooled Stepped Spillways

The quantification of the energy dissipation performance and residual energy is important for design purposes. For all stepped configurations, the residual energy was calculated at the chute downstream end on the basis of air-water flow measurements with the double-tip conductivity probe. The residual energy $H_{res}$ was calculated from the energy equation:

$$H_{res} = \int_0^{Y_{90}} (1-C) \times \cos\theta \times dy + \frac{q_w^2}{2 \times g \times \left[\int_0^{Y_{90}} (1-C) \times dy\right]^2} + w \tag{10}$$

The data of the present study are illustrated in dimensionless terms $H_{res}/d_c$ as a function of the dimensionless discharge $d_c/h$ in Fig. 9. Some further air-water flow data on flat and pooled stepped spillways were reanalyzed and compared with the present data in Fig. 9: Thorwarth (2008) with $\theta = 14.6°$, $h = 5$ cm, $w = 1$ to 5 cm and Kökpinar (2004) with $\theta = 30°$, $h = 6$ cm, and $w = 3$ cm. For the stepped chute with $\theta = 26.6°$, the residual head was smallest for the flat stepped spillway in the skimming flow regime compared with the corresponding pooled stepped spillway. In contrast, the residual energy on the stepped spillway with $\theta = 8.9°$ and the reanalyzed data of Thorwarth (2008) showed some smaller residual heads for the pooled stepped spillways, whereas the dimensionless residual head remained almost constant for the investigated discharges. The reanalyzed data of Kökpinar (2004) yielded some much larger residual energy for both flat and pooled stepped spillways ($\theta = 30°$). The physical explanation for the larger values of $H_{res}/d_c$ for the data of Kökpinar (2004) is unknown. However, the residual head for the flat stepped spillway was smaller for all discharges. This observation was in agreement with the findings in the present study of smaller residual head for the flat stepped spillway with similar channel slope ($\theta = 26.6°$). Some further flat and pooled step configurations with $\theta = 30°$ were investigated on different stepped spillway models by Takahashi et al. (2008) and André (2004). Takahashi et al. (2008) and André (2004) did not measure the energy dissipation performances on the basis of air-water flow properties, and the comparison was only able to be made qualitatively. The results by both Takahashi et al. (2008) and André (2004) showed little difference in energy dissipation performance between the flat and pooled step data. Overall, the present analysis implied that the chute slope had a large impact on the residual energy for both flat and pooled stepped spillways. On the stepped slopes (26.6° and 30°), smaller residual energy was achieved on the flat stepped spillway configuration, whereas the

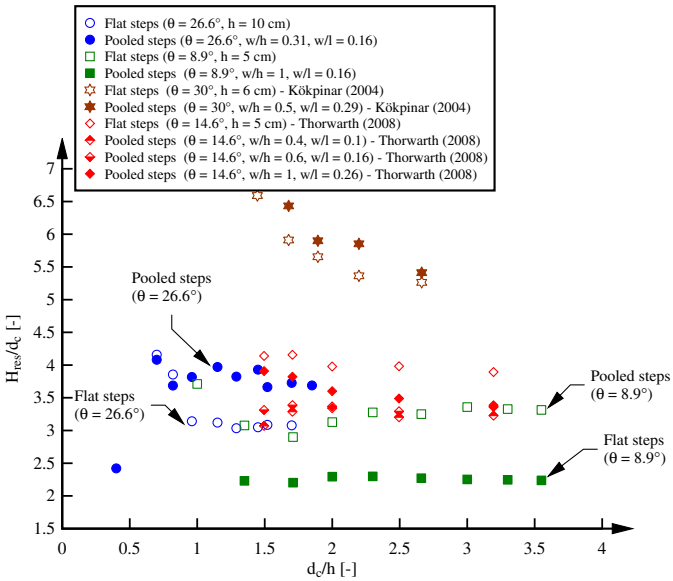


**Fig. 9.** Comparison of dimensionless residual head at the downstream end on the flat and pooled stepped spillways; comparison with reanalyzed data of Kökpinar (2004) and Thorwarth (2008); transition and skimming flow data

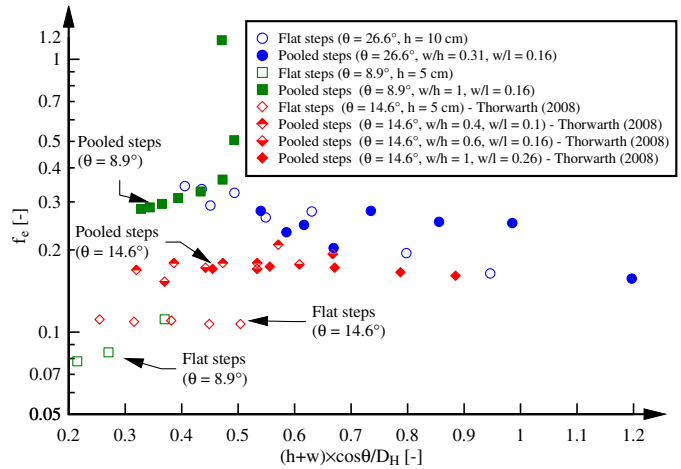


**Fig. 10.** Comparison of Darcy friction factors on the flat and pooled stepped spillways; comparison with reanalyzed data of Thorwarth (2008); transition and skimming flow data

residual energy was smaller for the pooled stepped spillway configuration on the slopes with 8.9° and 14.6°. For the pooled stepped spillways with slopes of 14.6° and 8.9°, some instabilities existed which might have enhanced the energy dissipation performance.

For design engineers, the flow resistance is a characteristic parameter, and the Darcy friction $f_e$ factor was calculated for gradually-varied flow in the air-water flow region (Chanson et al. 2002):

$$f_e = \frac{8 \times \tau_0}{\rho_w \times U_w^2} = \frac{8 \times g \times S_f \times d}{U_w^2} \quad (11)$$

where $U_w$ = flow velocity ($U_w = q_w/d$); the friction slope equals $S_f = -\partial H/\partial x$; and $x$ = distance in flow direction (Henderson 1966; Chanson 2001). The equivalent Darcy friction factors for the present flat and pooled step configurations were compared with some reanalyzed data by Thorwarth (2008) in Fig. 10 as a function of the dimensionless step cavity roughness height $(h + w) \times \cos\theta/D_H$, where $D_H$ is the hydraulic diameter or equivalent pipe diameter. All data for the stepped spillways with $\theta = 26.6°$ showed some scatter within $0.15 < f_e < 0.28$ for skimming flows. There was no clear trend in terms of flow resistance. Larger friction factors were observed for smaller flow rates $f_e = 0.3$. On the stepped chutes with slopes $\theta = 8.9°$ and $\theta = 14.6°$, the friction factors were significantly smaller on the flat stepped spillways compared with the pooled steps. That is, the friction factor on the flat stepped spillways was $f_e = 0.1$. For the pooled stepped spillways with $\theta = 14.6°$, $f_e = 0.19$, whereas $f_e \geq 0.3$ on the 8.9° slope pooled stepped spillway (Fig. 10). For the pooled stepped spillway with $\theta = 8.9°$, the larger friction factors were observed for the transition flow regimes, which exhibited the strong instationary air-water flows. On the stepped chute with $\theta = 26.6°$, the pool weir did not enhance the flow resistance, contrary to the flat slope observations, although the rate of pool weir height to step length were identical. The pool weirs on the stepped spillway with $\theta = 26.6°$ showed little effect on the friction factors despite some data scatter. Although the weir did not affect the flow resistance for the slope of 26.6°, it would be interesting to investigate the effect of larger weir height on the energy dissipation rate and the flow resistance for the same channel slope. The observations in the present study agreed with the friction factor measurements in a homogenous flow by André (2004) on a flat and pooled stepped spillway with $\theta = 30°$, showing little difference between flat and pooled steps.

## Conclusions

Experiments were conducted on pooled stepped spillways with slopes of 8.9° and 26.6° and the corresponding flat steps for a range of discharges. The flow patterns exhibited some instabilities on the pooled stepped spillways linked with some pulsations in the first pool cavity. The pulsations caused some small instabilities of the nappe flows for the 26.6° sloped stepped chute. The transition flow regime on the 8.9° pooled stepped spillway showed much stronger instabilities, with some jump waves propagating downstream. The air-water flow properties agreed with some self-similar equations in terms of interfacial velocity $V/V_{90}$ and void fractions. However, the distribution of dimensionless interfacial velocity $V/V_c$ showed smaller velocity on the pooled steps for $\theta = 8.9°$ compared with the flat steps and comparatively larger velocities for the pooled steps for $\theta = 26.6°$. For both channel slopes, some differences were also observed in terms of the bubble count rate and turbulence intensities. The comparative analysis suggested some smaller residual energy on the pooled stepped spillway with $\theta = 8.9°$ compared with the flat steps, whereas the residual energy on the 26.6° slope stepped chute was larger on the pooled steps compared with the flat steps. The differences in energy dissipation behavior for the two channel slopes were supported by reanalyzed data on pooled stepped spillways with $\theta = 14.6°$ and $\theta = 30°$. Although the pooled stepped spillway with $\theta = 8.9°$ appeared best in terms of energy dissipation, some strong hydrodynamic self-sustained instabilities were observed affecting the safe operation of the chute. The finding illustrates that some thorough physical modeling is required for complex stepped spillway designs.

## Acknowledgments

The authors thank Professor Holger Schüttrumpf (IWW, RWTH Aachen University) for providing access to the experimental facility and Jason Van Der Gevel and Stewart Matthews (The University

of Queensland) for their technical assistance. The financial supports through a UQ research scholarship and through the Australian Research Council (Grant DP120100481) are acknowledged.

## Notation

*The following symbols are used in this paper:*

$C$ = void fraction or air content;
$C_{mean}$ = mean air concentration;
$D_H$ = hydraulic diameter (m);
$D_o$ = dimensionless constant function of the depth-averaged air concentration;
$d$ = equivalent clear-water flow depth (m);
$d_c$ = critical flow depth (m);
$F$ = bubble count rate (Hz);
$\mathsf{F}^*$ = Froude number defined in terms of the step roughness;
$f_e$ = equivalent Darcy friction factor;
$g$ = gravity acceleration constant ($m/s^2$);
$H$ = total head (m);
$H_{res}$ = residual energy (m);
$h$ = step height (m);
$K'$ = dimensionless integration constant;
$K^*$ = dimensionless constant;
$k_s$ = step cavity height (m);
$L_I$ = longitudinal distance (m) from weir crest to inception point of free-surface aeration;
$l$ = step length (m);
$l_w$ = pool weir length (m);
$N$ = exponent;
$q_w$ = water discharge per unit width ($m^2/s$);
$S_f$ = friction slope;
Tu = turbulence intensity;
$U_w$ = mean flow velocity (m/s);
$V$ = interfacial velocity (m/s);
$V_c$ = critical flow velocity (m/s);
$V_{90}$ = interfacial velocity where $C = 90\%$ (m/s);
$W$ = channel width (m);
$w$ = pool weir height (m);
$x$ = flow direction;
$Y_{90}$ = characteristic flow depth where $C = 90\%$;
$y$ = direction normal to the pseudobottom formed by the step edges;
$\Delta x$ = longitudinal separation between probe tips (m);
$\Delta z$ = transverse separation between probe tips (m);
$\theta$ = channel slope;
$\rho$ = density ($kg/m^3$);
$\tau_0$ = shear stress (Pa); and
Ø = diameter of probe tips (m).

## References

André, S. (2004). "High velocity aerated flows on stepped chutes with macro-roughness elements." Ph.D. thesis, Laboratoire de Constructions Hydraulics (LCH), EPFL, Lausanne, Switzerland.

Carosi, G., and Chanson, H. (2006). "Air-water time and length scales in skimming flow on a stepped spillway. Application to the spray characterisation." *Rep. No. CH59/06*, Division of Civil Engineering, Univ. of Queensland, Brisbane, Australia.

Chanson, H. (1995). "Air bubble entrainment in free-surface turbulent flows. Experimental investigations." *Rep. CH46/95*, Dept. of Civil Engineering, Univ. of Queensland, Brisbane Australia.

Chanson, H. (2001). *The hydraulics of stepped chutes and spillways*, Balkema, Lisse, Netherlands.

Chanson, H., and Toombes, L. (2002a). "Energy dissipation and air entrainment in stepped storm waterway: Experimental study." *J. Irrig. Drain. Eng.*, 128(5), 305–315.

Chanson, H., and Toombes, L. (2002b). "Air-water flows down stepped chutes: Turbulence and flow structure observations." *Int. J. Multiphase Flow*, 28(11), 1737–1761.

Chanson, H., Yasuda, Y., and Ohtsu, I. (2002). "Flow resistance in skimming flows and its modelling." *Can. J. Civil Eng.*, 29(6), 809–819.

Ditchey, E. J., and Campbell, D. B. (2000). "Roller compacted concrete and stepped spillways." *Int. Workshop on Hydraulics of Stepped Spillways*, Balkema, Leiden, Netherlands, 171–178.

Felder, S. (2013). "Air-water flow properties on stepped spillways for embankment dams: Aeration, energy dissipation and turbulence on uniform, non-uniform and pooled stepped chutes." Ph.D. thesis, School of Civil Engineering, Univ. of Queensland, Brisbane, Australia.

Felder, S., and Chanson, H. (2012a). "Free-surface profiles, velocity and pressure distributions on a broad-crested weir: A physical study." *J. Irrig. Drain. Eng.*, 138(12), 1068–1074.

Felder, S., and Chanson, H. (2012b). "Air-water flow measurements in instationary free-surface flows: A triple decomposition technique." *Hydraulic Model Rep. No. CH85/12*, School of Civil Engineering, Univ. of Queensland, Brisbane, Australia.

Felder, S., Fromm, C., and Chanson, H. (2012a). "Air entrainment and energy dissipation on a 8.9° slope stepped spillway with flat and pooled steps." *Hydraulic Model Rep. No. CH86/12*, School of Civil Engineering, Univ. of Queensland, Brisbane, Australia.

Felder, S., Guenther, P., and Chanson, H. (2012b). "Air-water flow properties and energy dissipation on stepped spillways: A physical study of several pooled stepped configurations." *Hydraulic Model Rep. No. CH87/12*, School of Civil Engineering, Univ. of Queensland, Brisbane, Australia.

Hansen, K. D., and Reinhardt, K. D. (1991). *Roller-compacted concrete dams*, McGraw-Hill, New York.

Henderson, F. M. (1966). *Open channel flow*, MacMillan, New York.

Hunt, S., and Kadavy, K. (2013). "Inception point for embankment dam stepped spillways." *J. Hydraul. Eng.*, 139(1), 60–64.

Kökpinar, M. A. (2004). "Flow over a stepped chute with and without macro-roughness elements." *Can. J. Civil Eng.*, 31(5), 880–891.

Meireles, I., and Matos, J. (2009). "Skimming flow in the nonaerated region of stepped spillways over embankment dams." *J. Hydraul. Eng.*, 135(8), 685–689.

Takahashi, M., Yasuda, Y., and Ohtsu, I. (2008). "Flow patterns and energy dissipation over various stepped chutes. discussion." *J. Irrig. Drain. Eng.*, 134(1), 114–116.

Thorwarth, J. (2008). "Hydraulisches Verhalten der Treppengerinne mit eingetieften Stufen—Selbstinduzierte Abflussinstationaritäten und Energiedissipation [Hydraulics of pooled stepped spillways—Self-induced unsteady flow and energy dissipation]." Ph.D. thesis, Univ. of Aachen, Aachen, Germany (in German).

Toombes, L. (2002). "Experimental study of air-water flow properties on low-gradient stepped cascades." Ph.D. thesis, Dept. of Civil Engineering, Univ. of Queensland, Brisbane, Australia.

Toombes, L., and Chanson, H. (2008). "Flow patterns in nappe flow regime down low gradient stepped chutes." *J. Hydraul. Res.*, 46(1), 4–14.